Engineering Substrate Preference in Subtilisin: Structural and Kinetic Analysis of a Specificity Mutant[†]

Biao Ruan, Viktoriya London, Kathryn E. Fisher, D. Travis Gallagher, and Philip N. Bryan*

Center for Advanced Research in Biotechnology, University of Maryland Biotechnology Institute, 9600 Gudelsky Drive, Rockville, Maryland 20850

Received January 16, 2008; Revised Manuscript Received April 30, 2008

ABSTRACT: Bacillus subtilisin has been a popular model protein for engineering altered substrate specificity. Although some studies have succeeded in increasing the specificity of subtilisin, they also demonstrate that high specificity is difficult to achieve solely by engineering selective substrate binding. In this paper, we analyze the structure and transient state kinetic behavior of Sbt160, a subtilisin engineered to strongly prefer substrates with phenylalanine or tyrosine at the P4 position. As in previous studies, we measure improvements in substrate affinity and overall specificity. Structural analysis of an inactive version of Sbt160 in complex with its cognate substrate reveals improved interactions at the S4 subsite with a P4 tyrosine. Comparison of transient state kinetic behavior against an optimal sequence (DFKAM) and a similar, but suboptimal, sequence (DVRAF) reveals the kinetic and thermodynamic basis for increased specificity, as well as the limitations of this approach. While highly selective substrate binding is achieved in Sbt160, several factors cause sequence specificity to fall short of that observed with natural processing subtilisins. First, for substrate sequences which are nearly optimal, the acylation reaction becomes faster than substrate dissociation. As a result, the level of discrimination among these substrates diminishes due to the coupling between substrate binding and the first chemical step (acylation). Second, although Sbt160 has 24-fold higher substrate affinity for the optimal substrate DFKAM than for DVRAF, the increased substrate binding energy is not translated into improved transition state stabilization of the acylation reaction. Finally, as interactions at subsites become stronger, the rate-determining step in peptide hydrolysis changes from acylation to product release. Thus, the release of the product becomes sluggish and leads to a low k_{cat} for the reaction. This also leads to strong product inhibition of substrate turnover as the reaction progresses. The structural and kinetic analysis reveals that differences in the binding modes at subsites for substrates, transition states, and products are subtle and difficult to manipulate via straightforward protein engineering. These findings suggest several new strategies for engineering highly sequence selective enzymes.

Subtilisin BPN′ from *Bacillus amyloliquefaciens* is a secreted, serine protease which degrades proteins in the extracellular environment of the bacillus (*1–3*). Bacillus subtilisins have evolved to be highly efficient, hydrolyzing a broad spectrum of protein substrates at turnover rates exceeding 10^6 M^{-1} s^{-1} at 25 °C (*4*). Although most bacterial and fungal subtilisins have a degradative function, some eukaryotic subtilisins are highly specific processing enzymes. These subtilisins process prohormones into mature hormones by cleaving precisely at highly specific, cognate sequences (*5*). The ability to engineer a degradative subtilisin into a processing enzyme would be important both technologically and for understanding how natural, sequence-specific proteases regulate hormone metabolism, as well as other physiological processes (*6*). Consequently, many studies have focused on altering the substrate specificity of subtilisin (*7*).

Most subtilisin contacts are made with the first four substrate residues on the acyl side of the scissile bond. These are denoted P1−P4, numbering from the scissile bond toward the N-terminus of the substrate (*8–10*). The backbone of the substrate inserts between strands 100−104 and 125−129 of subtilisin to become the central strand in an antiparallel β-sheet arrangement involving seven main chain H-bonds (*9, 11*). The side chain components of substrate binding to subtilisin result primarily from the P1, P2, and P4 amino acids (*4, 12, 13*) (Figure 1). Accordingly, most mutations affecting specificity have been made in binding pockets S1 (*12, 14–27*), S2 (*6, 28–30*), and S4 (*31–38*).

Although many of these studies have succeeded in producing subtilisin variants with increased specificity, they also demonstrate that high specificity is difficult to achieve by engineering selective substrate binding alone. In this paper, we analyze the structure and transient state kinetic behavior of a subtilisin engineered to strongly prefer substrates with phenylalanine or tyrosine at the P4 position. These experiments show the effects of P4−S4 interactions on microscopic rate constants and reveal why high selectivity is difficult to achieve by engineering improved subsite interactions.

[†] This work was supported by NIH Grant GM42560.

* To whom correspondence should be addressed. E-mail: bryan@umbi.umd.edu. Telephone: (240) 314-6220. Fax: (240) 314-6255.

10.1021/bi800089f CCC: $40.75
Published on Web 05/29/2008

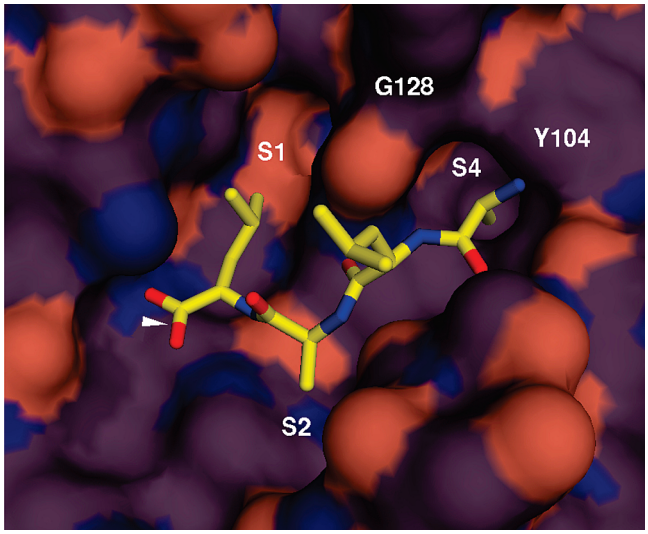

FIGURE 1: Wild-type active site region of subtilisin with peptide ligand. This structure was made using Protein Data Bank (PDB) entry 1SUA with bound tetrapeptide Ala-Leu-Ala-Leu (bright colors, foreground) bound to specificity pockets S1−S4 (background surface). Subsites S1, S2, and S4 are labeled. The S1 subsite is occupied by leucine, and the S4 subsite is occupied by alanine. The white triangle indicates the location of the scissile bond. Locations of wild-type residues Tyr 104 and Gly 128, which line the S4 pocket, are labeled. This image was made with PyMol using the 2.1 Å resolution crystal structure (*42*). This variant (1SUA, Sbt70) has a wild-type active site and S1−S4 subsites like Sbt149, except that it contains the inactivating mutation S221A to facilitate crystallization.

METHODS

Expression and Purification of Subtilisins. The subtilisin gene from *B. amyloliquefaciens* (subtilisin BPN′) has been cloned, sequenced, and expressed at high levels from its natural promoter sequences in *Bacillus subtilis* (*2, 3*). All mutant genes were recloned into a pUB110-based expression plasmid and used to transform *B. subtilis*. The *B. subtilis* strain used as the host contains a chromosomal deletion of its subtilisin gene and therefore produces no background wild-type activity (*39*). Subtilisin variants Sbt149[1] and Sbt160 were expressed in a 1.5 L New Brunswick fermentor at a level of ≥200 mg/L. After fermentation,16 g of Tris base and 22 g of $CaCl_2$ (dihydrate) were added to ∼1400 mL of broth. Cells and precipitate were pelleted in 250 mL bottles by centrifugation at 12000*g* for 30 min at °C. Acetone (70% final volume) was added to the supernatant. The 70% acetone mixture was then centrifuged in 500 mL bottles at 12000*g* for 30 min at 4 °C. The pellet was resuspended in ∼150 mL of 20 mM HEPES (pH 7.0) and 1 mM $CaCl_2$. Resuspended material was centrifuged at 12000*g* for 10 min at 4 °C to remove insoluble material. Using a vacuum funnel, the sample was passed over 150 g of DE52, equilibrated in 20 mM HEPES (pH 7.0). The DE52 was washed twice with 150 mL of 20 mM HEPES, 1 mM $CaCl_2$ buffer, and the all washes were pooled. Solid NH_4SO_4 was added to the sample to a final concentration of 1.8 M. Final purification was carried out using a 2 cm × 30 cm Poros HP 20 column on a Biocad Sprint. The sample was loaded and washed in 1.8 M NH_4SO_4 and 20 mM HEPES (pH 7.0) and then eluted with a linear gradient [1.8 to 0 M NH_4SO_4 in 20 mM HEPES (pH 7.0)] (*40*). The [E] was determined using an $E_{0.1\%}$ of 1.15 at 280 nm (*1, 41*). Purity was assessed by SDS−PAGE and estimated to be ∼95%.

Kinetic Measurements. Succinyl-DVRAF-7-amino-4-methylcoumarin (sDVRAF-AMC) and succinyl-DFKAM-7-amino-4-methylcoumarin (sDFKAM-AMC) were purchased from AnaSpec, Inc. Succinyl-AAPF-7-amino-4-methylcoumarin (sAAPF-AMC) was purchased from Sigma. Concentrations of the AMC substrates were determined by absorbency at 324 nm using an extinction coefficient of 16 mM^{-1} cm^{-1}. Reaction kinetics of AMC substrates were measured using a KinTek stopped-flow model SF2001 instrument (excitation, 380 nm; emission, 400 nm cutoff filter). A stock solution of enzyme at a concentration of 2 mM in 10 mM KP_i (pH 5.7), 100 mM NaCl, and 50% glycerol was prepared for kinetic studies. Immediately prior to stop-flow mixing, enzyme was diluted into 100 mM Tris-HCl (pH 8.6), 200 mM NaCl, and 0.2 mM EDTA and placed in syringe A of the SF2000 instrument. A solution of the substrate in water was placed in syringe B. Solutions were equilibrated at 22 °C. Fluorescence data were collected after 1:1 mixing of the two solutions. For measurement of single-turnover kinetics, the final enzyme concentration was varied from ∼2 to ∼60 μM with a constant substrate concentration, as specified in the figure legends. For measurement of burst kinetics, the final substrate concentration was varied from 1.5 to 25 μM with a constant enzyme concentration of 0.4−0.7 μM. At least 10 kinetic traces were collected for each experiment. Kinetic mechanisms were simulated using KinTek Global Explorer which was purchased from KinTek Corp.

Crystallization and Structure Analysis. The structure of PDB entry 1SUA (Sbt70, Figure 1) was determined as described previously (*42*). The structure of PDB entry 3CNQ (Sbt164, Figure 2) was obtained as follows. Purified enzyme with a stoichiometric amount of proenzyme at 9 mg/mL protein in 10 mM KCl was crystallized at room temperature by vapor diffusion in hanging drops using 15% PEG 8000, 0.2 M zinc acetate, and 0.1 M sodium cacodylate (pH 6.5) as a precipitant. Crystals grew as rectangular bars and belong to space group $P2_12_12_1$ with lattice constants of 43.2, 72.9, and 93.1 Å. A diffraction data set 99% complete to 1.7 Å resolution with an R_{sym} of 0.06 was collected from one crystal at beamline 24ID at the Advanced Photon Source of Argonne National Laboratory. The structure was determined by molecular replacement using AMORE (*43*) and refined to a final R_{free} value of 0.23 using REFMAC5 (*44*) and XFIT (*45*). The final model contains all enzyme atoms except the first two residues (disordered) and all proenzyme atoms except residues 1−8. Coordinates and complete statistics are available from the RCSB Protein Data Bank as entry 3CNQ.

[1] Abbreviations: Sbt149, subtilisin from *B. amyloliquefaciens* with Q2K, S3C, P5S, S9A, I31L, K43N, M50F, A73L, Δ75−83, E156S, G166S, G169A, S188P, Q206C, N212G, K217L, N218S, S221A, T254A, and Q271E mutations; Sbt160, Sbt149 with Y104A and G128S mutations; Sbt164, Sbt160 with D32A and S221A mutations; PAGE, polyacrylamide gel electrophoresis; sAAPF-AMC, succinyl-L-Ala-L-Ala-L-Pro-L-Phe-7-amino-4-methylcoumarin; sDFKAM-AMC, succinyl-L-Asp-L-Phe-L-Lys-L-Ala-L-Met-7-amino-4-methylcoumarin; sDVRAF-AMC, succinyl-L-Asp-L-Val-L-Arg-L-Ala-L-Phe-7-amino-4-methylcoumarin; Tris, tris(hydroxymethyl)aminomethane. A shorthand for denoting amino acid substitutions employs the single-letter amino acid code as follows: N218S denotes the change of asparagine 218 to serine.

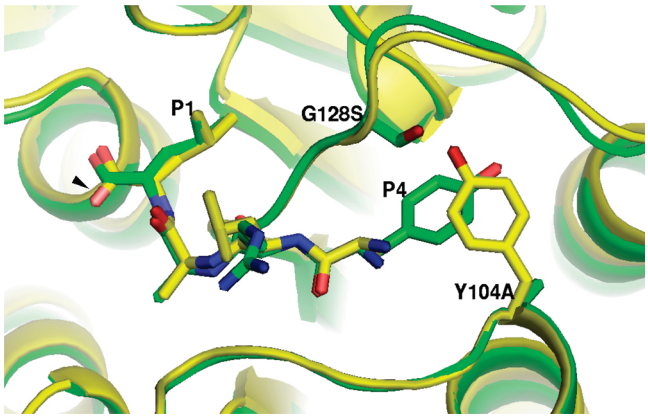

FIGURE 2: Overlay of the structure from Figure 1 (wild-type active site, yellow) and variant Sbt164 with the enlarged S4 pocket (green) produced by the mutations Y104A and G128S. The green structure also includes a ligand with Tyr-Arg-Ala-Leu bound in the P4−P1 positions. The black triangle indicates the position of the scissile bond. The proteins are represented by worms and ribbons, except for side chains at the mutation sites (104 and 128). The proteins and ligands superimpose closely, and the green Tyr P4 side chain fits into the enlarged S4 surface pocket between the two mutations. This image was made with PyMol using PDB entry 1SUA and 1.7 Å resolution PDB entry 3CNQ, which features Sbt164, an inactivated (D32A, S221A) form of Sbt160. The Sbt189 ligand (green) also includes an N-terminal extension that is not shown.

RESULTS AND DISCUSSION

Subtilisin Engineering. To engineer processing subtilisins, we needed to understand how subtilisin catalyzes the cleavage of substrates with a wide range of binding affinities. We began with characterization of a hyperstable and independently folding mutant (Sbt149): Q2K, S3C, P5S, S9A, I31L, K43N, M50F, A73L, Δ75−83, E156S, G166S, G169A, S188P, Q206C, N212G, K217L, N218S, T254A, and Q271E (*46*). Our long-term goal of engineering highly specific subtilisins necessitates introduction of potentially destabilizing mutations into the active site and substrate binding pockets. Using a hyperstable framework as a starting point allows us to introduce mutations which would otherwise cause difficulties in expression and purification (*47*). Optimal substrates for Sbt149 are similar to wild-type subtilisin. Preferred substrates have F, L, I, or V at P4 (*4, 36*), A or S at P2 (*4, 16*), and Y, F, L, or M at P1 (*4, 12*).

Figure 1 shows the arrangement of the key specificity-determining pockets S1, S2, and S4 in subtilisin 1SUA, which like Sbt149 has a wild-type active site, except that the active site serine 221 is mutated to alanine to inactivate the enzyme and facilitate crystallization. This structure also contains a tetrapeptide ligand, ALAL, with alanine in the S4 pocket and leucine in the S1 pocket. The S1 pocket is clearly larger than necessary to bind the P1 leucine, and more importantly, the S4 pocket also has additional capacity, somewhat occluded behind the Tyr 104 residue. This additional capacity in S4 is the basis for the wild type's ability to turn over substrates with Phe at P4 slightly faster than substrates with Ala at P4.

Engineering of the S4 Pocket To Increase Substrate Binding Specificity. To narrow the substrate specificity of Sbt149, we enlarged the S4 binding pocket. This decision was based on many earlier studies which examined the effects of S4 mutations on specificity. The natural preference of subtilisin for a P4 amino acid is as follows: F > L ∼ V ∼ I > A (*32, 34–36*). The preference for F relative to A is 3-fold for substrates where kinetic coupling is weak (*33, 35*). Rheinnecker et al. (*35*) have previously noted that expanding the S4 pocket can result in a significant increase in specificity by affecting both K_M and k_{cat}. They suggested that the expanded S4 cavity causes structural changes which are propagated to the active site. Optimal active site geometry is restored by filling the cavity with a bulky P4 hydrophobe. Consequently, the mutations G128S and Y104A were introduced into Sbt149, producing the variant Sbt160.

Table 1: Steady State Parameters for Sbt149 and Sbt160

	K_M (μM)	k_{cat} (s^{-1})	k_{cat}/K_M (M^{-1} s^{-1})
	Sbt149		
sAAPF-AMC	125	35	0.28×10^6
sDVRAF-AMC	2.3	26	11.1×10^6
sDFKAM-AMC	0.6	7.4	12.5×10^6
	Sbt160		
sAAPF-AMC[a]	—	—	900
sDVRAF-AMC	156	16	0.1×10^6
sDFKAM-AMC	0.8	1.3	1.7×10^6

[a] K_M and k_{cat} could be accurately determined for Sbt160 with sAAPF-AMC because of an inability to reach saturation.

Figure 2 shows the resulting structure, with a ligand featuring a P4 tyrosine bound in the S4 binding pocket, superimposed on the wild-type ALAL complex of Figure 1. The P4 tyrosine side chain overlaps slightly with the former position of Tyr 104, now mutated to Ala, and fits snugly below the new Ser 128 side chain. The P4 tyrosine appears to form favorable contacts in the enlarged S4 pocket, including numerous van der Waals interactions.

Comparison of the Specificities of Sbt149 and Sbt160. We analyzed the steady state behavior of Sbt149 and Sbt160 versus three peptide substrates: sAAPF-AMC, sDVRAF-AMC, and sDFKAM-AMC. AMC is a fluorogenic leaving group enabling amide bond cleavage to be followed by fluorescence. sAAPF-AMC can be considered an average substrate for Sbt149 (*48*). It has a preferred amino acid (F) at the S1 site and average amino acids at the S4 and S2 sites. sDVRAF-AMC is a preferred substrate for Sbt149, having preferred amino acids at P1 (F), P2 (A), and P4 (V). sDFKAM-AMC is also a preferred substrate for Sbt149 but was chosen in particular because it should also be a fully optimized substrate for Sbt160. Steady state kinetic parameters for the three substrates with the two subtilisins are listed in Table 1. The standard condition for these and all subsequent assays includes 50 mM Tris-HCl (pH 8.6), 100 mM NaCl, and 0.1 mM EDTA at 22 °C.

The k_{cat}/K_M of Sbt149 for sDVRAF-AMC is 40-fold higher than for sAAPF-AMC. Sbt149 has little discrimination between sDVRAF-AMC and sDFKAM-AMC: k_{cat}/K_M = 11.1×10^6 and 12.5×10^6 M^{-1} s^{-1}, respectively. An upper limit of turnover in this range has previously been observed for natural subtilisin BPN′ with good substrates (*13, 46*). The k_{cat}/K_M of Sbt160 versus sAAPF-AMC (900 M^{-1} s^{-1}) is ∼1.900-fold lower than that for sDFKAM-AMC (1.7×10^6 M^{-1} s^{-1}), indicating that sAAPF-AMC [an average substrate for Sbt149 (Table 1)] is a very poor substrate for Sbt160. Further, the k_{cat}/K_M of Sbt160 versus sDVRAF-AMC is 17 times lower than that for sDFKAM-AMC, indicating that the expanded S4 pocket increased the level of discrimination between an optimal sequence and a similar, but

Scheme 1

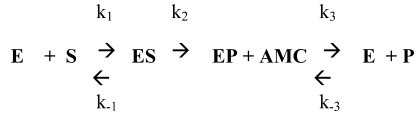

suboptimal, sequence. Comparison of k_{cat}/K_M values allows quantitation of substrate preferences but does not reveal the kinetic and thermodynamic basis for the preference (*49*). To improve our understanding of specificity, we employed transient state kinetic methods to determine microscopic rate constants.

Transient State Kinetic Analysis. (1) Pre-Steady State Kinetics. A minimal kinetic scheme for subtilisin catalysis is shown in Scheme 1: where E is the enzyme, S the substrate, and P the peptide product. Pre-steady state experiments were performed for Sbt149 and Sbt160 with sAAPF-AMC, sDVRAF-AMC, and sDFKAM-AMC. In these experiments, subtilisin (0.4−1 μM) was mixed with 3−25 μM substrate in a stopped-flow fluorescence instrument. No pre-steady state burst phase is observed for Sbt149 with sAAPF-AMC or for Sbt160 with either sAAPF-AMC or sDVRAF-AMC. Thus, for these substrate−enzyme combinations, the time dependence for formation of cleaved product is linear and obeys steady state approximations:

$$K_M \sim (k_{-1} + k_2)/k_1 \text{ and } k_{cat} \sim k_2$$

Burst kinetics are observed for Sbt149 with sDVRAF-AMC and sDFKAM-AMC and for Sbt160 with sDFKAM-AMC. The time dependence for formation of free AMC is described by a rapid exponential phase followed by a linear phase. The kinetics are described by

$$[\text{product}]/[\text{Sbt}] = A_o(1 - e^{-\lambda t}) + k_{cat}t$$

The rate constants are defined by the equations $\lambda \sim k_2 + k_3$ and $k_{cat} \sim k_2k_3/(k_2 + k_3)$. The amplitude of the burst phase (A_o) $\sim [k_2/(k_2 + k_3)]^2$.

Representative burst kinetics are shown for Sbt149 and Sbt160 with sDFKAM-AMC in Figure 3. The pre-steady state analysis shows that the rate-determining step in peptide hydrolysis can change from acylation to product release as interactions at subsites become stronger.

(2) Single-Turnover Kinetics. Single-turnover experiments were performed for Sbt149 and Sbt160 with sAAPF-AMC, sDVRAF-AMC, and sDFKAM-AMC. Kinetics were determined as a function of [Sbt] (in excess of substrate) to determine microscopic rate constants for a single pass through the catalytic cycle. [Sbt] was varied from 2 to 60 μM with [substrate] fixed at 1 μM. Representative single-turnover kinetics are shown for Sbt149 with sDFKAM-AMC (Figure 4) and Sbt160 with sDFKAM-AMC (Figure 5). The kinetic curves are biphasic with the fast phase determined by $k_1[E] + k_{-1} + k_2$. A plot of rate versus [Sbt] of the major kinetic phase approximates a hyperbole determined by $k_2k_1[E]/(k_1[E] + k_2 + k_{-1})$ (*49*).

For Sbt149 and Sbt160 with sDFKAM-AMC, the pre-steady state and single-turnover experiments clearly show that the acylation reaction occurs much faster than product release. The slow product release could be due to slow deacylation (k_3), slow dissociation of the sDFKAM peptide product from the enzyme (k_4), or a combination of both. A more detailed kinetic scheme for subtilisin catalysis is shown in Scheme 2: where E is the enzyme, S the substrate, EA the acyl−enzyme intermediate, and P the peptide product. To separate the kinetic components involved in product release, product inhibition of Sbt149 and Sbt160 by sAAFP, sDVRAF, and sDFKAM was assessed. Inhibition constants were calculated using global kinetic analysis software because product binding and dissociation cannot be assumed to be in rapid equilibrium with other species. For tight binding product−enzyme combinations, both product on (k_{-4}) and off (k_4) rates could be extracted from the fitting. Once these parameters were determined, all microscopic constants in Scheme 2 could be determined with reasonable certainty for Sbt149 with sDVRAF-AMC and sDFRAM-AMC and for Sbt160 with sDFRAM-AMC. All experimental data for these combinations were fit according to Scheme 2 using KinTek Global Explorer and are given in Table 2. For Sbt149, the acylation rate increases in the following order: sAAPF-AMC < sDVRAF-AMC < sDFKAM-AMC. The rates of deacylation and product dissociation fall, however. For Sbt149 and sDFKAM-AMC, the rate of product release is slower than the deacylation rate. For Sbt160, acylation rates are similar for sDVRAF-AMC and sDFKAM-AMC, but the deacylation rate for sDFKAM falls to 1.8 s^{-1} and is the slowest step in the reaction pathway. Since deacylation is limiting the overall reaction rate, we tested whether k_{cat} would increase in the presence of a strong exogenous nucleophile such as hydroxylamine (*50*). Consequently, steady state measurements were carried out for Sbt160 with sDFKAM-AMC with 0.2−0.9 M hydroxylamine. We observed that k_{cat} decreases by ~50% as the hydroxylamine concentration is increased to 0.9 M. Unfortunately, the result neither supports nor refutes our kinetic model because deacylation and product release occur at similar rates. Further, the decrease in k_{cat} versus hydroxylamine concentration may indicate that dissociation of the amide product generated by the hydroxylamine reaction is slower than dissociation of the acid product generated by hydrolysis.

Assessment of Success and Prospects for Improvement. The k_{cat}/K_M of Sbt160 for sDFKAM-AMC is 17 times greater than for sDVRAF-AMC. By this measure, the engineering of the S4 pocket to improve specificity for an optimal versus a similar sequence could be called a success because the parent subtilisin (Sbt149) does not discriminate at all between the two substrates. As a practical matter, however, Sbt160 is not sufficiently specific to be a useful processing protease. The crucial question is how one does better. Steady state kinetic measurements allow one to measure specificity but provide limited insight into the thermodynamic and kinetic basis for specificity. The reason for this is that K_M and k_{cat} are composite rate constants into which are folded multiple microscopic rate constants for the multistep hydrolysis reaction. It frequently is assumed for subtilisins that $k_{cat} \sim k_2$ and $K_M \sim K_S$. These relationships are accurate only if k_2 is small compared to k_{-1}, k_3, and k_4, however. While this is true with average and poor substrates, it is not true with the preferred substrates. As subsite interactions "improve", k_2 can become larger than k_{-1}, k_3, and k_4. As k_2 approaches k_{-1}, substrate binding can no longer be viewed as a rapid equilibrium which is kinetically uncoupled from acylation. This has important consequences for specificity. Specificity is defined here as the ratio of k_{cat}/K_M of an enzyme for one substrate relative to another. The k_{cat}/K_M value is the apparent

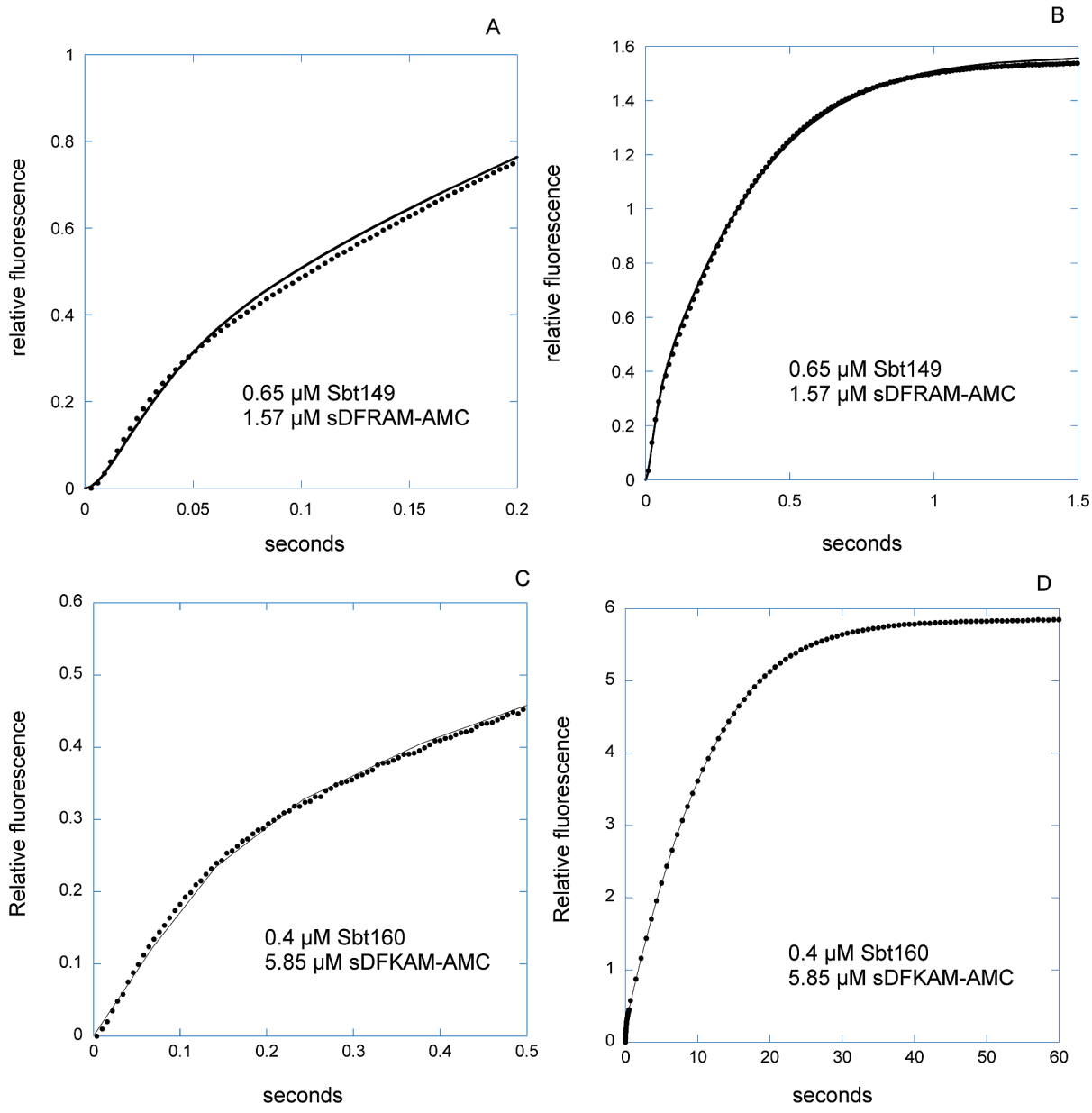

FIGURE 3: Pre-steady state kinetics of Sbt149 and Sbt160 vs sDFKAM-AMC. The [AMC]/[enzyme] ratio is plotted vs time after mixing with enzyme (●). (A and B) [Sbt149] = 0.65 μM with 1.57 μM sDFKAM-AMC. (C and D) [Sbt160] = 0.4 μM with 5.85 μM sDFKAM-AMC. Reactions were carried out at 22 °C. Solid lines are fits to Scheme 2 obtained with KinTek Global Explorer.

Scheme 2

$$E + S \underset{k_{-1}}{\overset{k_1}{\rightleftarrows}} ES \xrightarrow{k_2} EA + AMC \xrightarrow{k_3} EP \underset{k_{-4}}{\overset{k_4}{\rightleftarrows}} E + P$$

second-order rate constant for productive substrate binding. It is less than the true binding rate (k_1) by a factor of $k_2/(k_{-1} + k_2)$ (*49*). As k_{-1} slows to less than the acylation rate and the enzyme begins to reach a maximum level determined by the rate of substrate binding, the coefficient $k_2/(k_{-1} + k_2)$ approaches 1. Thus coupling between substrate binding and acylation (the first chemical step) broadens specificity. To create a higher-specificity subtilisin, both substrate affinity and kinetic coupling need to be considered. Further, as product release becomes slower than acylation, it determines the k_{cat} of the reaction rather than the acylation rate.

Thus, determination of microscopic rate constants allows us to make a more rigorous assessment of the kinetic basis for a change in specificity and reveals five basic challenges to engineering increased sequence specificity and potential solutions. Below the data for Sbt160 are discussed and compared to transient state kinetic data for a natural processing subtilisin (Kex2) from yeast (*51, 52*).

(1) Discrimination at the Level of Substrate Binding. Expanding the S4 binding pocket with the Y104A and G128S mutations results in a K_S for sDFKAM-AMC of 6.6 μM, 24 times tighter than that for sDVRAF-AMC. By comparison, the K_S of Kex2 for a cognate sequence is ~25 μM (*51*). The ability of Kex2 to discriminate between a cognate P4 (norleucine) and a noncognate (alanine) on the basis of differential substrate affinity is 10-fold. By this measure, the engineering of the S4 pocket in Sbt160 to improve specificity for a cognate versus a near-cognate sequence could be called a success.

(2) Kinetic Coupling of Substrate Binding and Acylation. For Sbt160 and a cognate substrate (sDFKAM-AMC), k_{-1} equals

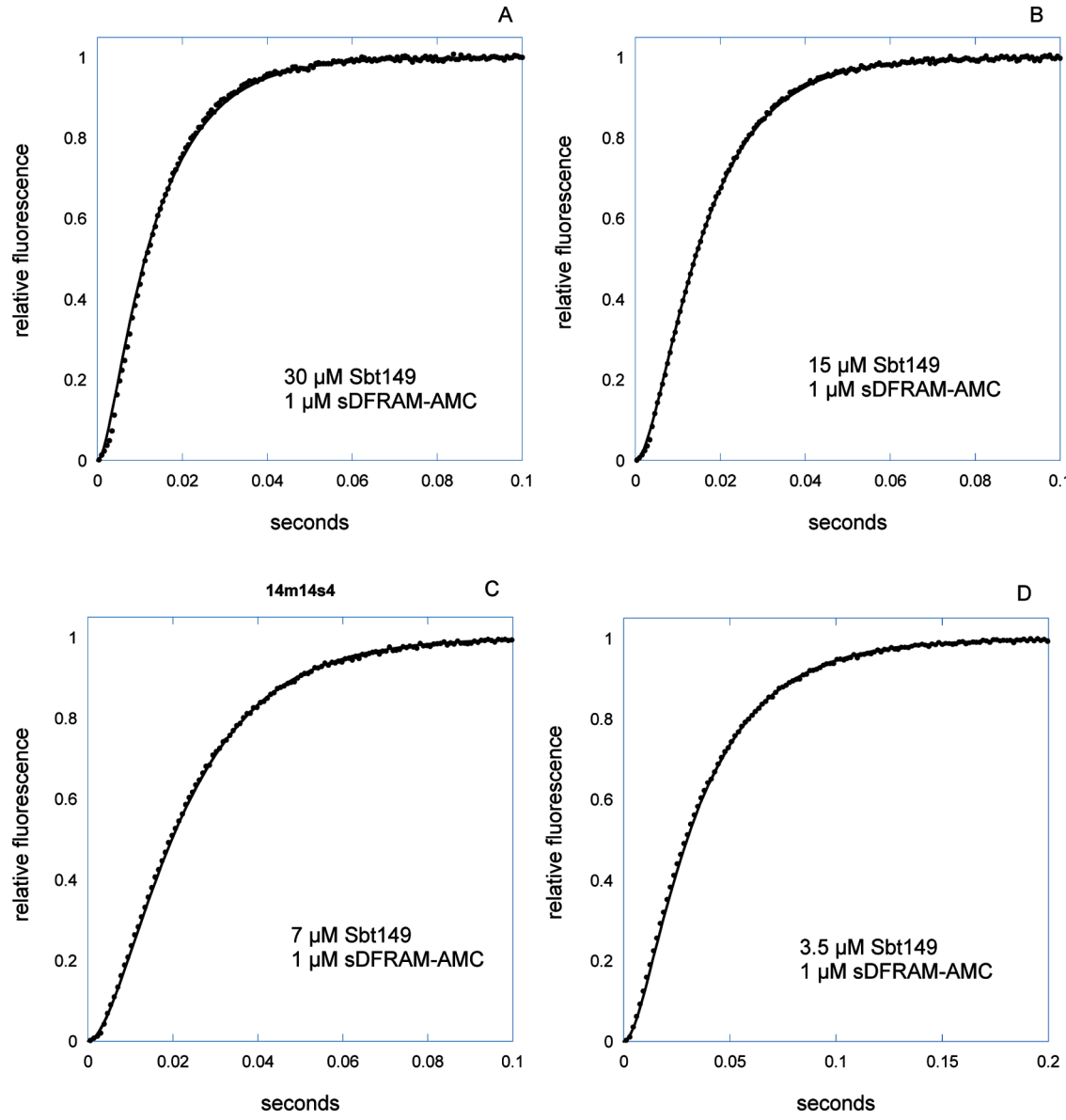

FIGURE 4: Single-turnover kinetics of Sbt149 vs sDFKAM-AMC. Sbt149 at 30 (A), 15 (B), 7 (C), and 3.5 μM enzyme (D) was mixed with 1 μM sDFKAM-AMC. The release of AMC is followed by fluorescence for each Sbt149 concentration (●). Reactions were carried out at 22 °C. Solid lines are fits to Scheme 2 obtained with KinTek Global Explorer.

$2k_2$. This kinetic coupling causes the substrate binding rate as well as substrate affinity to influence the overall rate of the reaction and broadens specificity (*53*). For sDVRAF-AMC, $k_{cat} \sim k_2$ and $K_M \sim K_S$, so the binding and acylation reactions are not coupled. Surprisingly, kinetic coupling also appears to exist with Kex2 (*51*). The acylation rate with a cognate arginine at P1 can exceed 500 s^{-1}, a value which is likely in the same range as the rate of substrate dissociation (*54*). In the case of Kex2, however, rapid acylation is observed only with a cognate amino acid at P1, and hence, noncognate sequences are kinetically uncoupled.

(3) Acylation Reaction. Although Sbt160 has better substrate affinity for sDFKAM-AMC than sDVRAF-AMC, the improved substrate binding energy does not translate into improved transition state stabilization of the acylation reaction. The acylation rates of Sbt160 for sDVRAF-AMC (16.5 s^{-1}) and sDFRAM-AMC (18 s^{-1}) are very similar. This contrasts with Kex2 and other processing subtilisins such as furin (*45*). Acylation rates are very fast with cognate substrates and dramatically fall with near-cognate sequences. One reason for this is that substrate binding and transition state stabilization are dependent on the binding of calcium in the S1 pocket of Kex2 and furin (*55, 56*). Cofactor-dependent catalysis appears to tightly link substrate binding energy to transition state stabilization.

(4) Deacylation Reaction. The rate-determining step in peptide hydrolysis changes from acylation to deacylation as interactions at subsites become stronger. The engineered S4 pocket appears to preferentially stabilize the acyl intermediate of sDFRAM. This is a major deficiency in Sbt160. Deacylation of near-cognate and noncognate sequences is faster than deacylation for the cognate sequence. Since deacylation is the rate-limiting step in hydrolysis of the cognate sequence, k_{cat} is sluggish (1.3 s^{-1}). Deacylation is also the rate-limiting step in the catalytic cycle of Kex2 with a cognate sequence (*52*). Unlike Sbt160, however, deacylation with a cognate P4 amino acid is as fast as for a noncognate P4 amino acid.

(5) Product Inhibition. The product sDFKAM binds strongly to both Sbt149 and Sbt160, causing strong inhibition of substrate turnover as the reaction progresses. An unin-

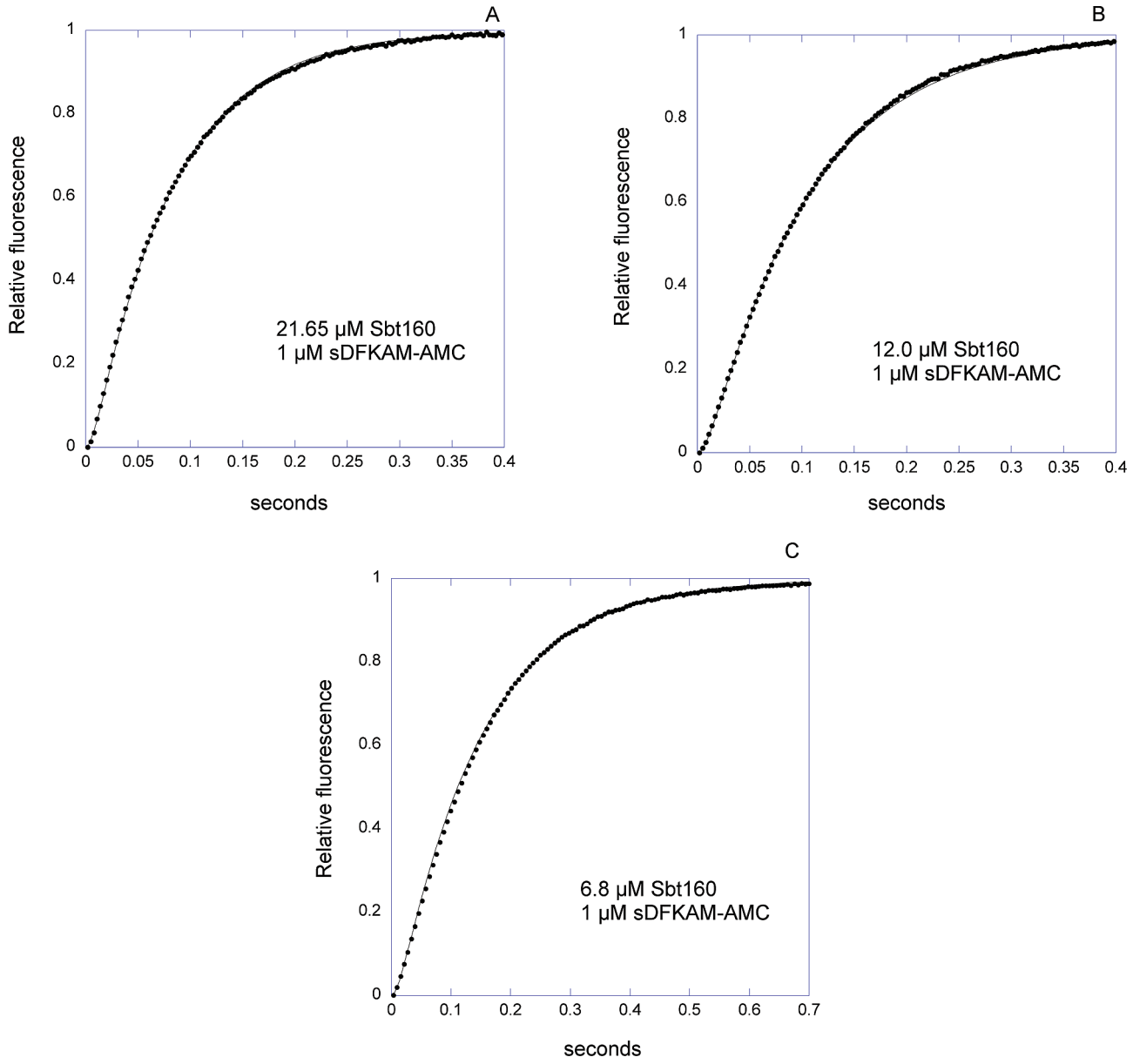

FIGURE 5: Single-turnover kinetics of Sbt160 vs sDFKAM-AMC. Sbt160 at 21.65 (A), 12.0 (B), and 6.8 μM enzyme (C) was mixed with 1 μM sDFKAM-AMC. Reactions were carried out at 22 °C. The release of AMC is followed by fluorescence for each Sbt160 concentration (●). Solid lines are fits to Scheme 2 obtained with KinTek Global Explorer.

Table 2: Transient State Kinetic Analysis pf Sbt149 and Sbt160[a]

	k_1 (M^{-1} s^{-1})	k_{-1} (s^{-1})	k_2 (s^{-1})	k_3 (s^{-1})	k_4 (s^{-1})	k_{-4} (M^{-1} s^{-1})	K_S (μM)	K_P (μM)
				Sbt149				
sDVRAF-AMC	2.1×10^7	55	65	60	160	2.0×10^7	2.7	8
sDFKAM-AMC	1.4×10^7	12	82	21	13	1.4×10^7	0.8	0.9
				Sbt160				
sDFKAM-AMC	4.6×10^6	31	18	1.8	6	4.6×10^7	6.6	1.3

[a] Microscopic rate constants could not be determined for the other enzyme−substrate pairs for which $K_M \sim K_S$ and $k_{cat} \sim k_2$.

tended consequence of engineering the S4−P4 interaction was altering the balance between substrate affinity (K_S = 6.6 μM) and product affinity (K_P = 1.3 μM) in Sbt160. Sbt149 binds the sDFKAM-AMC substrate with the approximately same affinity as the peptide product (~1 μM).

Thus, transient state kinetic analysis reveals a critical deficiency in our engineering approach: differences in the binding modes at subsites for substrates, transition states, and products are subtle and difficult to manipulate via straightforward protein engineering (*53*). However, the analysis and comparison with Kex2 suggest that an indirect approach, by engineering a substrate-dependent cofactor site, could be more successful. In recent work, we have used this insight to engineer highly specific processing subtilisins by making chemical steps dependent on substrate sequence through the formation of an anion site. A first-generation cofactor-dependent subtilisin has been described previously (*47*). We have been able to apply the principles described

above to create subtilisins which are both highly active (in the presence of an activating cofactor) and highly specific due to linkage of substrate binding and cofactor binding (B. Ruan et al., manuscript in preparation).

ACKNOWLEDGMENT

We thank Edward Eisenstein, Lizbeth Hedstrom, and James Stivers for helpful discussion. We also thank reviewers for helpful suggestions. Instruments and products are identified in this paper solely to specify the experimental procedure and not to imply recommendation or endorsement.

REFERENCES

1. Ottesen, M., and Svendsen, I. (1970) The Subtilisins. *Methods Enzymol. 19*, 199–215.
2. Wells, J. A., Ferrari, E., Henner, D. J., Estell, D. A., and Chen, E. Y. (1983) Cloning, sequencing and secretion of *Bacillus amyloliquifaciens* subtilisin in *Bacillus subtilis*. *Nucleic Acids Res. 11*, 7911–7925.
3. Vasantha, N., Thompson, L. D., Rhodes, C., Banner, C., Nagle, J., and Filpula, D. (1984) Genes for alkaline and neutral protease from *Bacillus amyloliquifaciens* contain a large open-reading frame between the regions coding for signal sequence and mature protein. *J. Bacteriol. 159*, 811–819.
4. Gron, H., Meldal, M., and Breddam, K. (1992) Extensive comparison of the substrate preferences of two subtilisins as determined with peptide substrates which are based on the principle of intramolecular quenching. *Biochemistry 31*, 6011–6018.
5. Steiner, D., Smeekens, S. P., Ohagi, S., and Chan, S. J. (1992) The new enzymology of precursor processing endoproteases. *J. Mol. Biol. 267*, 23435–23438.
6. Carter, P., and Wells, J. A. (1987) Engineering enzyme specificity by 905 substrate-assisted catalysis. *Science 237*, 394–399.
7. Leis, J. P., and Cameron, C. E. (1994) Engineering proteases with altered specificity. *Curr. Opin. Biotechnol. 5*, 403–408.
8. Berger, A., and Schechter, I. (1970) Mapping the active site of papain with the aid of peptide substrates and inhibitors. *Philos. Trans. R. Soc. London, Ser. B 257*, 249–264.
9. McPhalen, C. A., Schnebli, H. P., and James, M. N. (1985) Crystal and molecular structure of the inhibitor eglin from leeches in complex with subtilisin Carlsberg. *FEBS Lett. 188*, 55–58.
10. Bode, W., Papamokos, E., Musil, D., Seemueller, U., and Fritz, H. (1986) Refined 1.2 Å crystal structure of the complex formed between subtilisin Carlsberg and the inhibitor eglin c. Molecular structure of eglin and its detailed interaction with subtilisin. *Embo J 5*, 813–818.
11. McPhalen, C. A., and James, M. N. G. (1988) Structural comparison of two serine proteinase-protein inhibitor complexes: Eglin-C-Subtilisin Carlsberg and CI-2-Subtilisin novo. *Biochemistry 27*, 6582–6598.
12. Estell, D. A., Graycar, T. P., Miller, J. V., Powers, D. B., Burnier, J. P., Ng, P. G., and Wells, J. A. (1986) Probing steric and hydrophobic effects on enzyme-substrate interactions by protein engineering. *Science 233*, 659–663.
13. Gron, H., and Breddam, K. (1992) Interdependency of the binding subsites in subtilisin. *Biochemistry 31*, 8967–8971.
14. Wells, J. A., Powers, D. B., Bott, R. R., Graycar, T. P., and Estell, D. A. (1987) Designing substrate specificity by protein engineering of electrostatic interactions. *Proc. Natl. Acad. Sci. U.S.A. 84*, 1219–1223.
15. Wells, J. A., Cunningham, B. C., Graycar, T. P., and Estell, D. A. (1987) Recruitment of substrate-specificity properties from one enzyme into a related one by protein engineering. *Proc. Natl. Acad. Sci. U.S.A. 84*, 5167–5171.
16. Ballinger, M. D., Tom, J., and Wells, J. A. (1995) Designing subtilisin BPN′ to cleave substrates containing dibasic residues. *Biochemistry 34*, 13312–13319.
17. Mei, H. C., Liaw, Y. C., Li, Y. C., Wang, D. C., Takagi, H., and Tsai, Y. C. (1998) Engineering subtilisin YaB: Restriction of substrate specificity by the substitution of Gly124 and Gly151 with Ala. *Protein Eng. 11*, 109–117.
18. Takagi, H. (1992) [Protein engineering of subtilisin]. *Tanpakushitsu Kakusan Koso 37*, 303–313.
19. Takagi, H., Maeda, T., Ohtsu, I., Tsai, Y. C., and Nakamori, S. (1996) Restriction of substrate specificity of subtilisin E by introduction of a side chain into a conserved glycine residue. *FEBS Lett. 395*, 127–132.
20. Takagi, H., Yamamoto, M., Ohtsu, I., and Nakamori, S. (1998) Random mutagenesis into the conserved Gly154 of subtilisin E: Isolation and characterization of the revertant enzymes. *Protein Eng. 11*, 1205–1210.
21. Tanaka, T., Matsuzawa, H., Kojima, S., Kumagai, I., Miura, K., and Ohta, T. (1998) P1 specificity of aqualysin I (a subtilisin-type serine protease) from *Thermus aquaticus* YT-1, using P1-substituted derivatives of *Streptomyces* subtilisin inhibitor. *Biosci., Biotechnol., Biochem. 62*, 2035–2038.
22. DeSantis, G., Berglund, P., Stabile, M. R., Gold, M., and Jones, J. B. (1998) Site-directed mutagenesis combined with chemical modification as a strategy for altering the specificity of the S1 and S1′ pockets of subtilisin *Bacillus* lentus. *Biochemistry 37*, 5968–5973.
23. DeSantis, G., Shang, X., and Jones, J. B. (1999) Toward tailoring the specificity of the S1 pocket of subtilisin *B. lentus*: Chemical modification of mutant enzymes as a strategy for removing specificity limitations. *Biochemistry 38*, 13391–13397.
24. DeSantis, G., and Jones, J. B. (1999) Probing the altered specificity and catalytic properties of mutant subtilisin chemically modified at position S156C and S166C in the S1 pocket. *Bioorg. Med. Chem. 7*, 1381–1387.
25. Lu, W., Apostol, I., Qasim, M. A., Warne, N., Wynn, R., Zhang, W. L., Anderson, S., Chiang, Y. W., Ogin, E., Rothberg, I., Ryan, K., and Laskowski, M., Jr. (1997) Binding of amino acid side-chains to S1 cavities of serine proteinases. *J. Mol. Biol. 266*, 441–461.
26. Masuda-Momma, K., Shimakawa, T., Inouye, K., Hiromi, K., Kojima, S., Kumagai, I., Miura, K., and Tonomura, B. (1993) Identification of amino acid residues responsible for the changes of absorption and fluorescence spectra on the binding of subtilisin BPN′ and *Streptomyces* subtilisin inhibitor. *J. Biochem. 114*, 906–911.
27. Masuda-Momma, K., Hatanaka, T., Inouye, K., Kanaori, K., Tamura, A., Akasaka, K., Kojima, S., Kumagai, I., Miura, K., and Tonomura, B. (1993) Interaction of subtilisin BPN′ and recombinant *Streptomyces* subtilisin inhibitors with substituted P1 site residues. *J. Biochem. 114*, 553–559.
28. Carter, P., Nilsson, B., Burnier, J. P., Burdick, D., and Wells, J. A. (1989) Engineering Subtilisin BPN′ for site-specific proteolysis. *Proteins: Struct., Funct., Genet. 6*, 240–248.
29. Carter, P., Abrahmsen, L., and Wells, J. A. (1991) Probing the mechanism and improving the rate of substrate-assisted catalysis in Subtilisin BPN′. *Biochemistry 30*, 6141–6148.
30. Tanaka, T., Matsuzawa, H., and Ohta, T. (1998) Engineering of S2 site of aqualysin I: Alteration of P2 specificity by excluding P2 side chain. *Biochemistry 37*, 17402–17407.
31. Bech, L. M., Sorensen, S. B., and Breddam, K. (1992) Mutational replacements in subtilisin 309. Val104 has a modulating effect on the P4 substrate preference. *Eur. J. Biochem. 209*, 869–874.
32. Bech, L. M., Sorensen, S. B., and Breddam, K. (1993) Significance of hydrophobic S4-P4 interactions in subtilisin 309 from *Bacillus lentus*. *Biochemistry 32*, 2845–2852.
33. Gron, H., Bech, L. M., Sorensen, S. B., Meldal, M., and Breddam, K. (1996) Studies of binding sites in the subtilisin from *Bacillus lentus* by means of site directed mutagenesis and kinetic investigations. *Adv. Exp. Med. Biol. 379*, 105–112.
34. Sorensen, S. B., Bech, L. M., Meldal, M., and Breddam, K. (1993) Mutational replacements of the amino acid residues forming the hydrophobic S4 binding pocket of subtilisin 309 from *Bacillus lentus*. *Biochemistry 32*, 8994–8999.
35. Rheinnecker, M., Baker, G., Eder, J., and Fersht, A. R. (1993) Engineering a novel specificity in subtilisin BPN′. *Biochemistry 32*, 1199–1203.
36. Rheinnecker, M., Eder, J., Pandey, P. S., and Fersht, A. R. (1994) Variants of subtilisin BPN′ with altered specificity profiles. *Biochemistry 33*, 221–225.
37. Teplyakov, A. V., van der Laan, J. M., Lammers, A. A., Kelders, H., Kalk, K. H., Misset, O., Mulleners, L. J., and Dijkstra, B. W. (1992) Protein engineering of the high-alkaline serine protease PB92 from *Bacillus alcalophilus*: Functional and structural consequences of mutation at the S4 substrate binding pocket. *Protein Eng. 5*, 413–420.

38. Ballinger, M. D., Tom, J., and Wells, J. A. (1996) Furilisin: A variant of subtilisin BPN′ engineered for cleaving tribasic substrates. *Biochemistry 35*, 13579–13585.
39. Fahnestock, S. R., and Fisher, K. E. (1987) Protease-deficient *Bacillus subtilis* host strains for production of staphylococcal protein A. *Appl. Environ. Microbiol. 53*, 379–384.
40. Alexander, P. A., Ruan, B., Strausberg, S. L., and Bryan, P. N. (2001) Stabilizing mutations and calcium-dependent stability of subtilisin. *Biochemistry 40*, 10640–10644.
41. Pantoliano, M. W., Whitlow, M., Wood, J. F., Dodd, S. W., Hardman, K. D., Rollence, M. L., and Bryan, P. N. (1989) Large increases in general stability for Subtilisin BPN′ through incremental changes in the free energy of unfolding. *Biochemistry 28*, 7205–7213.
42. Almog, O., Gallagher, T., Tordova, M., Hoskins, J., Bryan, P., and Gilliland, G. L. (1998) Crystal structure of calcium-independent subtilisin BPN′ with restored thermal stability folded without the prodomain. *Proteins 31*, 21–32.
43. Navaza, J. (2001) Implementation of molecular replacement in AMoRe. *Acta Crystallogr. D57*, 1367–1372.
44. Murshudov, G. N., Vagin, A. A., and Dodson, E. J. (1997) Refinement of macromolecular structures by the maximum-likelihood method. *Acta Crystallogr. D53*, 240–255.
45. McRee, D. E. (1999) XtalView/Xfit: A versatile program for manipulating atomic coordinates and electron density. *J. Struct. Biol. 125*, 156–165.
46. Strausberg, S. L., Ruan, B., Fisher, K. E., Alexander, P. A., and Bryan, P. N. (2005) Directed coevolution of stability and catalytic activity in calcium-free subtilisin. *Biochemistry 44*, 3272–3279.
47. Ruan, B., Fisher, K. E., Alexander, P. A., Doroshko, V., and Bryan, P. N. (2004) Engineering subtilisin into a fluoride-triggered processing protease useful for one-step protein purification. *Biochemistry 43*, 14539–14546.
48. DelMar, E., Largman, C., Brodrick, J., and Geokas, M. (1979) A sensitive new substrate for chymotrypsin. *Anal. Biochem. 99*, 316–320.
49. Johnson, K. A. (1992) Transient-state kinetic analysis of enzyme reaction pathways. *Enzymes 20*, 1–61.
50. Fersht, A. R., Blow, D. M., and Fastrez, J. (1973) Leaving group specificity in the chymotrypsin-catalyzed hydrolysis of peptides. A stereochemical interpretation. *Biochemistry 12*, 2035–2041.
51. Rockwell, N. C., Krysan, D. J., Komiyama, T., and Fuller, R. S. (2002) Precursor processing by kex2/furin proteases. *Chem. Rev. 102*, 4525–4548.
52. Rockwell, N. C., and Fuller, R. S. (2001) Direct measurement of acylenzyme hydrolysis demonstrates rate-limiting deacylation in cleavage of physiological sequences by the processing protease Kex2. *Biochemistry 40*, 3657–3665.
53. Hedstrom, L. (2002) Serine protease mechanism and specificity. *Chem. Rev. 102*, 4501–4524.
54. Rockwell, N. C., and Fuller, R. S. (2001) Differential utilization of enzyme-substrate interactions for acylation but not deacylation during the catalytic cycle of Kex2 protease. *J. Biol. Chem. 276*, 38394–38399.
55. Holyoak, T., Wilson, M. A., Fenn, T. D., Kettner, C. A., Petsko, G. A., Fuller, R. S., and Ringe, D. (2003) 2.4 Å resolution crystal structure of the prototypical hormone-processing protease Kex2 in complex with an Ala-Lys-Arg boronic acid inhibitor. *Biochemistry 42*, 6709–6718.
56. Henrich, S., Cameron, A., Bourenkov, G. P., Kiefersauer, R., Huber, R., Lindberg, I., Bode, W., and Than, M. E. (2003) The crystal structure of the proprotein processing proteinase furin explains its stringent specificity. *Nat. Struct. Biol. 10*, 520–526.

BI800089F